



# EVALUATION OF A METASURFACE LINER CONCEPT FOR BROADBAND ACOUSTIC ABSORPTION

Victor Lafont<sup>1\*</sup>

Rémi Roncen<sup>1</sup>

Fabien Méry<sup>1</sup>

Delphine Sebbane<sup>1</sup>

<sup>1</sup> ONERA/DMPE, Université de Toulouse,  
F-31055 Toulouse - France

## ABSTRACT

Acoustic liners are the classical solution to reduce noise in aircraft turbofan engines. They consist in a array of resonant cavities topped by a resistive perforated sheet and work on the principle of a resonator. The desire for fuel-efficient aircrafts has led to the development of high bypass-ratio engines with less available space for acoustic treatments and larger fans that create a more broadband and low-frequency noise. New concepts of acoustic liners able to absorb over a large range of frequencies while taking even less space are therefore needed. The goal of the present work is to propose such a concept and assess its acoustic behavior. An innovative liner concept has been designed to provide a large range of attenuation while keeping a reasonable height, using the OPAL software developed at ONERA. A sample was then manufactured and tested under grazing flow and high sound levels in the B2A test bench. An inverse impedance eduction method then allows to compare the predicted and measured impedances.

**Keywords:** *Liner, Eduction, Impedance, Grazing flow.*

## 1. INTRODUCTION

Conventional, single degree of freedom (SDOF) liners consist of a honeycomb structure topped with a thin perforated facesheet, forming a layout of small resonators closed at their bottom by a rigid backplate. The geometry

of the honeycomb can be adjusted to match specific noise damping requirements [1]. The driving parameter for the noise damping power of locally reacting liners is their acoustic impedance, a complex number that is the ratio between acoustic pressure  $p$  and normal acoustic velocity  $v_n$  taken on the facesheet, normalized by the impedance of air  $\rho_0 c_0$ :

$$\zeta(\omega) = \frac{p}{\rho_0 c_0 v_n} = r(\omega) + j\chi(\omega), \quad (1)$$

where  $r$  and  $\chi$  are respectively called the resistance and the reactance of the liner.

For absorbing noise over a wide frequency range or at low frequencies, non-conventional liners like variable-depth liners or perforated plates connected to tubes of varying lengths may be necessary [2, 3]. In these cases, an optimization process using numerical and experimental tools is required to propose configurations that meet the necessary constraints. ONERA developed a software platform called OPAL to optimize complex meta-surface liners based on both conventional and non-conventional architectures. In this work, OPAL is used to design an innovative acoustic liner with a wide absorption range and test it under realistic experimental conditions. Section 2 briefly outlines the design process, including constraints, optimization, and fabrication of a sample. Section 3 presents the experimental setup used to measure the sample's acoustic response. Section 4 details the results and is followed by a short conclusion.

\*Corresponding author: victor.lafont@onera.fr

**Copyright:** ©2023 The authors. This is an open-access article distributed under the terms of the Creative Commons Attribution 3.0 Unported License, which permits unrestricted use, distribution, and reproduction in any medium, provided the original author and source are credited.



## 2. SAMPLE DESIGN

The goal is to propose a material with high absorption both in the low and high-frequency ranges. Since these two frequency objectives are generally antagonistic, a multi-objective optimization was conducted (see [4] for more details on the general process).

12 different liner architectures ranging from classical SDOF to multi-layer metasurfaces were numerically tested to find the best design for the proposed objectives, using the OPAL liner optimization tool developed at ON-ERA. For all designs, the maximum total thickness was set to 6 cm. Among the 12 proposed architectures, the one that offered the best compromise between all objectives while staying a relatively simple design is a single-layer metasurface of 9 parallel resonator cells of varying depth, with some of the cells based on the LEONAR concept (Long Elastic Open Neck Acoustic Resonator; see Refs [2, 5]). The cells are arranged in a square pattern and the total dimensions of the pattern are chosen so that they are far inferior to the target wavelengths to ensure impedance homogenization [4]. The assembly is topped by a wiremesh and a thin perforated sheet, with a tiny air gap left between the surface of the resonator cells and the wiremesh, to help mitigate grazing flow effects [6, 7]. Apart from the wiremesh and the perforated top plate which are both metallic, the sample is made using stereolithography (SLA) 3D-printing.

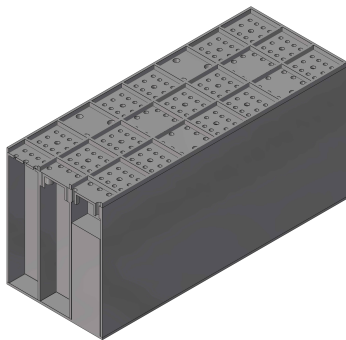


**Figure 1.** CAD of the metasurface cells

## 3. EXPERIMENTAL SETUP

This section briefly describes the experimental setup used. More details on the facilities and methods can be found in previous papers [8–10].

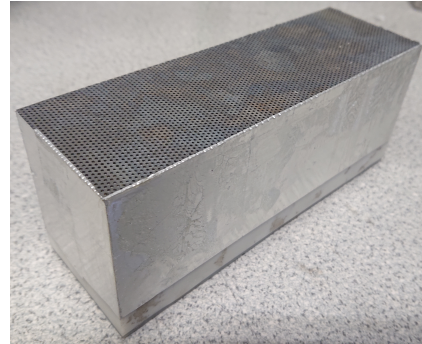


**Figure 2.** Complete assembly of the sample with top perforated plate

### 3.1 B2A Bench

The B2A is a test bench designed for acoustic measurements in the presence of grazing flow. It has a square section of side  $a = 50$  mm and has a quasi-anechoic termination. The test section is 200 mm long and is equipped with 17 microphone ports on its upper wall for acoustic pressure measurements. The samples are located on the lower wall of the test section and are 150 mm in length and 50 mm in width.

Recently an upgrade of the bench was done, so that two sets of two speakers can be placed upstream and downstream of the test section. It allows the generation of an acoustic wave propagating either with or against the flow depending on which set is used. The total level of the acoustic wave can reach 150 dB.

All measurements and analyses are performed under the assumption of plane waves since the frequencies used in the acoustic excitation are below the cut-off frequency of the duct.

### 3.2 Test matrix

With the aim of fully characterizing the behavior of the liner design, a number of measurements with varying grazing flow speeds and incident sound pressure levels (SPL) were conducted, in the upstream and downstream acoustic excitation setups. Table 1 sums up all the conditions used. The SPL indicated is the frequency-averaged incident SPL, obtained via a wavesorting method.

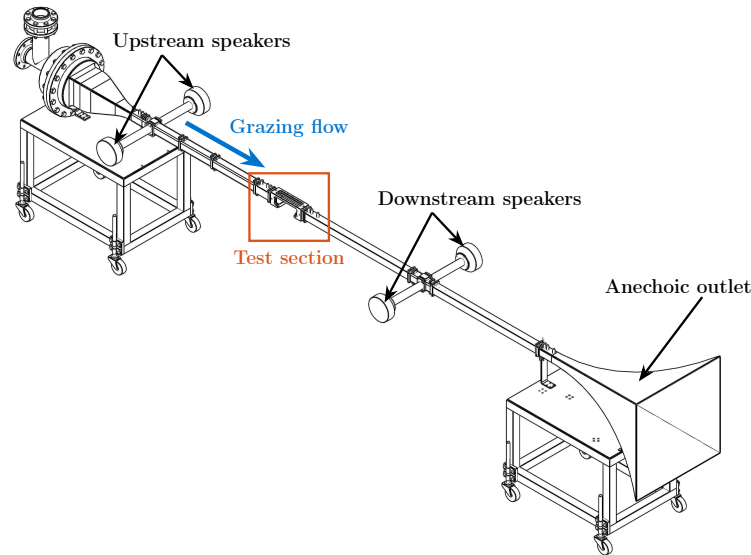


**Figure 3.** Sketch of the B2A bench

**Table 1.** Summary of performed measurements

Acoustic excitation	Bulk Mach $M_b$	SPL (dB)
Swept sine, upstream	0	110
		125
		130
		135
	0.1	110
		125
Swept sine, downstream	0.2	135
	0.3	135
	0	135
Swept sine, downstream	0.1	135
	0.2	135
	0.3	135

### 3.2.1 Acoustic excitation

Previously, the acoustic excitations used in the B2A were either multitone sines or broadband signals. With the upgrade work has been conducted to add the possibility to use swept sine signals, since they allow to measure the response of the liner over a wide frequency range with

a better signal-to-noise ratio than a broadband excitation with a similar acoustic level. The swept sine used in this study is ranging from 300 Hz to 3.3 kHz in 59 seconds, as seen in Figure 4 that shows the spectrum measured at the most upstream microphone location.

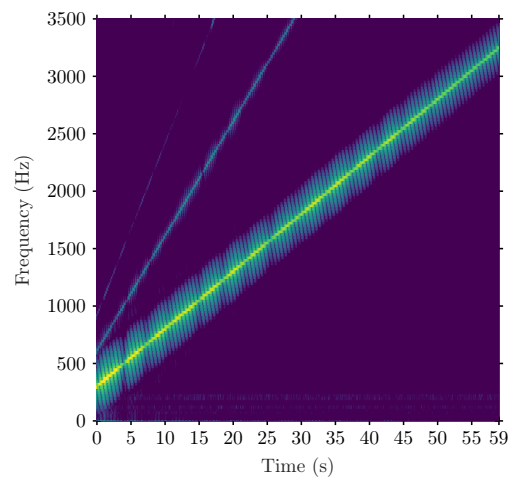


**Figure 4.** Spectrogram at the first upstream microphone position, no flow, SPL = 135 dB.

### 3.2.2 Impedance eduction

Impedance eduction is performed with OPAL using LEE (Linearized Euler equations) and a Direct Galerkin scheme [10, 11]. The shear flow profile at each bulk Mach number is taken into account in the eduction process. The selected profile is a generic flow profile (see Fig. 5) with a boundary layer thickness close to the experimental one measured by LDV; its exact shape has very little influence on the eduction results since the flow is fully developed.

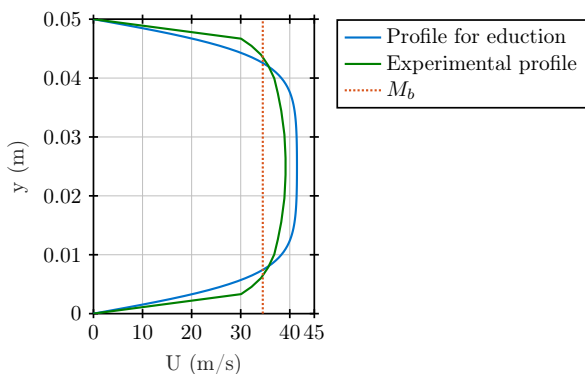


**Figure 5.** Example of flow profile at  $M_b = 0.1$ .

## 4. RESULTS AND DISCUSSION

This section presents the impedance eduction results. The eduction is performed for 120 evenly-spaced frequencies between 300 and 3300 Hz.

### 4.1 Influence of the incident acoustic level

Figure 6 shows the effect of an increase of the incident SPL on the educed resistance, with a fixed flow condition. The sample has a very linear behavior with respect to the SPL, both without flow and with grazing flow. This behavior was expected since both the LEONAR design and the wiremesh are known to be hardly sensitive to the effects of high sound levels [12, 13].

### 4.2 Influence of the grazing flow

Figures 7 and 8 show the eduction results for the cases at fixed high SPL (135 dB) and with upstream and downstream excitation respectively. We recall that in the case of upstream excitation, the acoustic wave propagates with the flow; while for downstream excitation, the acoustic

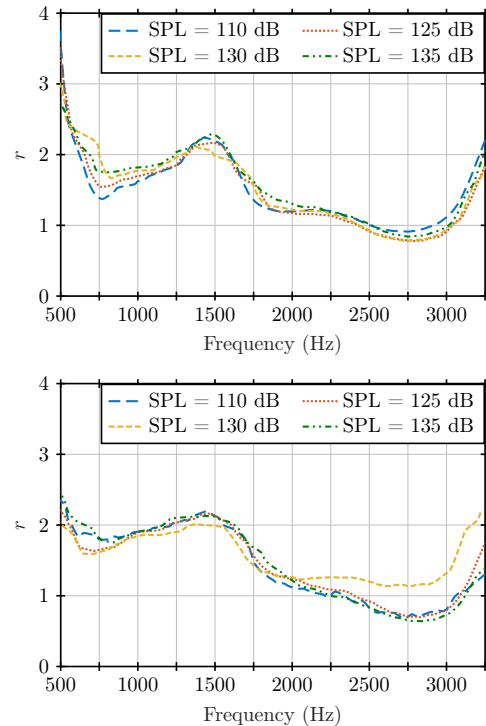


**Figure 6.** Educed resistance, upstream excitation,  $M_b = 0$  (top) and  $M_b = 0.1$  (bottom). SPL ranging from 110 to 135 dB.

wave propagates against the flow. The sample appears to be quite linear with respect to the grazing flow: the resistance is not modified significantly when  $M_b$  increases, except at higher frequencies in the upstream condition where the wiremesh might not be as effective as wished.

In both figures, the target impedance obtained with OPAL is plotted in solid purple lines. The agreement between expected and measured values is quite good around the maximum of absorption, where the reactance curve is flat and very close to being null. However, at higher frequencies (over 2 kHz), discrepancies appear for the resistance in the upstream excitation condition; these can be explained by the fact that the models for wiremesh behavior in OPAL are not taking into account all the grazing flow effects.

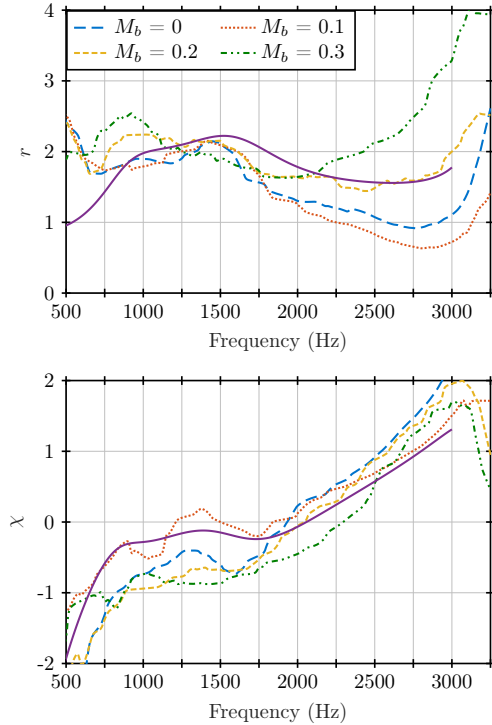


**Figure 7.** Educated resistance and reactance, upstream excitation, SPL = 135 dB. Solid line: OPAL predicted value at  $M_b = 0.3$

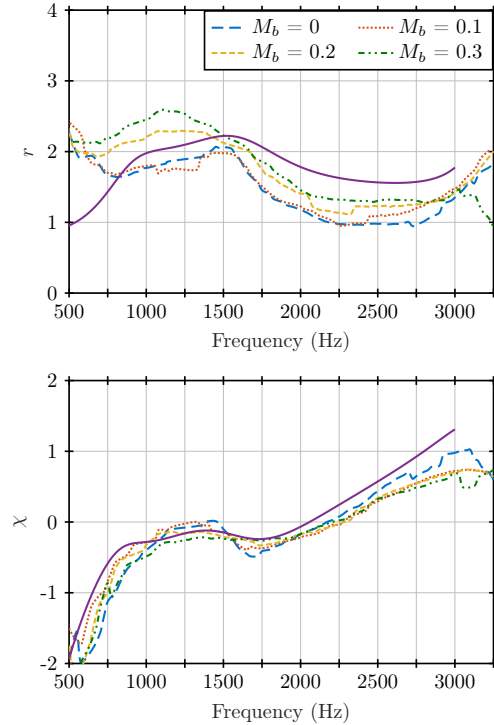


**Figure 8.** Educated resistance and reactance, downstream excitation, SPL = 135 dB. Solid line: OPAL predicted value at  $M_b = 0.3$

### 4.3 Comparison of acoustic excitations

Impedance education results with swept sine (at 135 dB) and broadband noise results obtained previously (with a SPL close to 140 dB) are compared in Fig. 9, in both upstream and downstream configurations at  $M_b = 0.3$ . The advantages of using a swept sine appear clearly: in these flow conditions the broadband noise is almost covered by the aerodynamic noise, leading to difficulties in the identification process, while the swept sine excitation emerges better and gives cleaner results. Nevertheless, the agreement between the values obtained with the two different types of excitations is quite good.

The differences observed in the upstream and downstream configurations with a swept sine excitation might be explained by the fact that sound absorption is higher in the downstream configuration, leading to better identification of the resistance in this case.

## 5. CONCLUSION

In this study, a specific optimization tool named OPAL developed at ONERA has proved its ability to propose innovative liner designs under several seemingly incompatible objectives. A sample has been made using the specs given by OPAL and tested under realistic grazing flow conditions in the B2A bench to obtain its impedance and compare it to the predicted value, using a swept sine excitation to emerge from the background aerodynamic noise better. The results of these tests showed that the prediction is very good, and that the newly tested swept sine excitation process is working as intended. The combined use of OPAL and grazing flow tests in the newly upgraded B2A is thus a promising way for future and even more complex liner designs.



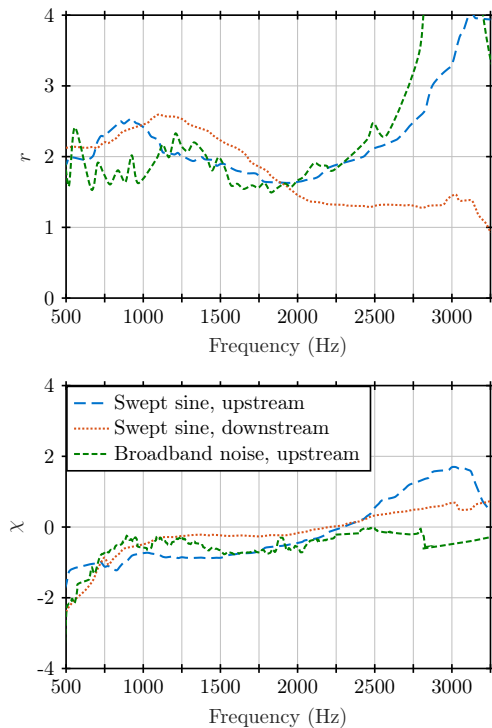


**Figure 9.** Comparison of the educed resistance and reactance with swept sine and broadband excitations,  $M_b = 0.3$ .

## 6. ACKNOWLEDGMENTS

The authors gratefully acknowledge Laurent Burel and Nicolas Fasano for the assembly of the new version of the B2A bench, as well as Ludovic Ambrosiani for his work on the swept sine excitation and Estelle Piot for the fruitful discussions during the writing of this paper.

This work was carried out in the framework of the MAMBO project, supported by the French Civil Aviation Agency (DGAC), the "France Relance" national recovery plan, and the "Nextgeneration EU" European recovery plan.

## 7. REFERENCES

- [1] R. E. Motsinger and R. E. Kraft, "Design and performance of duct acoustic treatment," *Aeroacoustics of Flight Vehicles: Theory and Practice. Volume 2: Noise Control*, 1991.
- [2] M. G. Jones, F. Simon, and R. Roncen, "Broadband and low-frequency acoustic liner investigations at NASA and ONERA," *AIAA Journal*, vol. 60, no. 4, pp. 2481–2500, 2022.
- [3] M. G. Jones, W. Watson, D. Nark, B. Howerton, and M. Brown, "A review of acoustic liner experimental characterization at NASA Langley," Apr. 2020.
- [4] R. Roncen, P. Vuillemin, P. Klotz, F. Simon, F. Méry, D. Sebbane, and E. Piot, "Design and optimization of acoustic liners with a shear grazing flow: OPAL software platform applications," in *INTER-NOISE and NOISE-CON Congress and Conference Proceedings*, vol. 263, pp. 152–163, Institute of Noise Control Engineering, 2021.
- [5] F. Simon, "Long Elastic Open Neck Acoustic Resonator for low frequency absorption," *Journal of Sound and Vibration*, vol. 421, pp. 1–16, 2018.
- [6] Y. Murata, T. Ishii, S. Enomoto, H. Oinuma, K. Nagai, J. Oki, and H. Daiguji, "Proposal of acoustic liners combined with fine-perforated-film," in *INTER-NOISE and NOISE-CON Congress and Conference Proceedings*, vol. 263, pp. 5475–5484, Institute of Noise Control Engineering, 2021.
- [7] Y. Murata, T. Ishii, S. Enomoto, H. Oinuma, K. Nagai, J. Oki, and H. Daiguji, "Experimental research on new acoustic liners combined with fine-perforated-film," in *28th AIAA/CEAS Aeroacoustics 2022 Conference*, p. 2885, 2022.
- [8] F. Méry, E. Piot, D. Sebbane, P. Reulet, F. Simon, and A. Carazo Méndez, "Experimental assessment of the effect of temperature gradient across an aeroacoustic liner," *Journal of Aircraft*, vol. 56, no. 5, pp. 1809–1821, 2019.
- [9] V. Lafont, F. Méry, R. Roncen, F. Simon, and E. Piot, "Liner impedance eduction under shear grazing flow at a high sound pressure level," *AIAA Journal*, vol. 58, no. 3, pp. 1107–1117, 2020.
- [10] V. Lafont, F. Méry, and F. Simon, "Liner multiphysics coupling between grazing flow, thermal gradients, and sound pressure levels," *AIAA Journal*, vol. 60, no. 8, pp. 4754–4763, 2022.
- [11] J. Primus, E. Piot, and F. Simon, "An adjoint-based method for liner impedance eduction: Validation and numerical investigation," *Journal of Sound and Vibration*, vol. 332, no. 1, pp. 58–75, 2013.

- [12] C. Yang, P. Zhang, S. Jacob, E. Trigell, and M. Åbom, “Investigation of extended-tube liners for control of low-frequency duct noise,” *AIAA Journal*, pp. 1–16, 2021.
- [13] X. Qiu, X. Jing, L. Du, J. Yang, X. Sun, and X. Zhang, “Nonlinear effect of wire mesh liners subjected to high sound pressure level,” *AIAA Journal*, vol. 60, no. 9, pp. 5521–5532, 2022.